Quasi-two-body decays $B_c \to K^* h \to K\pi h$ in perturbative QCD

Zi-Yu Zhang,[1] Zhi-Qing Zhang,[1,*] Si-Yang Wang,[2] Zhi-Jie Sun,[1] and You-Ya Yang[1]
[1]*Institute of Theoretical Physics, School of Sciences, Henan University of Technology, Zhengzhou, Henan 450052, China*
[2]*Institute of Particle Physics and Key Laboratory of Quark and Lepton Physics (MOE), Central China Normal University, Wuhan, Hubei 430079, China*

(Received 14 July 2023; accepted 26 September 2023; published 17 October 2023)

In this work, we study the quasi-two-body decays $B_c \to K^* h \to K\pi h (h = D, D_s, K, \pi, \eta, \eta')$ in the perturbative QCD (PQCD) approach. The two-meson distribution amplitudes $\Phi_{K\pi}^{\text{P-wave}}$ are introduced to describe the final-state interactions of the $K\pi$ pair, which involve the timelike form factors $F_{K\pi}(s)$ parametrized by the relativistic Breit-Wigner function and the Gegenbauer polynomials. We calculate the branching ratios for these quasi-two-body decays, from which one can obtain the branching ratios for the corresponding two-body decays under the narrow width approximation relation. We find that $B_c^+ \to K^{*+} D^0$ and $B_c^+ \to K^{*0} D^+$ have the largest branching ratios, which can reach up to 10^{-6}, while the branching ratios for other two-body decays are very small and only about $10^{-8} - 10^{-7}$. As we expected, the branching ratios of the pure annihilation decays are usually small, while in our considered such type of decays, the channel $B_c^+ \to \bar{K}^{*0} K^+$ has the largest branching ratio, which is near 10^{-6}. These results are consistent with the previously PQCD calculations obtained in the two-body framework, which can be tested by future LHCb experiments. For the decays $B_c^+ \to K^{*+} D^0 \to K^0 \pi^+ D^0$, $B_c^+ \to K^{*0} D^+ \to K^+ \pi^- D^+$, and $B_c^+ \to \bar{K}^{*0} D_s^+ \to K^- \pi^+ D_s^+$, we also calculate their direct CP violations and find that $A_{CP}(B_c^+ \to K^{*+} D^0 \to K^0 \pi^+ D^0) = (-14.6^{+9.2}_{-1.1})\%$ is the largest one, which is possible measured by the present LHCb experiments. For the pure annihilation type decays, there is no CP violation, because only the tree operators are involved. Furthermore, we give the differential distributions of the branching ratios and the direct CP violations in the $K\pi$ invariant mass ω for the decays $B_c \to K^* D_{(s)} \to K\pi D_{(s)}$.

DOI: 10.1103/PhysRevD.108.076009

I. INTRODUCTION

In $B_{u,d,s,c}$ meson systems, the B_c meson is the only quark-antiquark bound state $(\bar{b}c)$ composed of both heavy quarks with different flavors. It can decay only via weak interaction, since the two flavor asymmetric quarks (b and c) cannot be annihilated into gluons (photons) via strong (electromagnetic) interaction. While each of the two heavy quarks can decay individually through the $b \to c(u), c \to s(d)$ transitions, and they can also annihilate through weak interaction, so the B_c meson has many rich decay channels, B_c meson decays provide an ideal platform to study the nonleptonic weak decays of heavy mesons, to test the standard model, and to search for new physics signals. In recent years, some experimental studies on B_c meson decays to multihadron final states, such as $B_c \to K^+ K^- \pi^+$ [1], $B_c \to J/\psi D^{(*)0} K^+, J/\psi D^{(*)+} K^{*0}$ [2], $B_c \to p\bar{p}\pi^+$ [3], and $B_c \to J/\psi \pi^+ \pi^- \pi^+, J/\psi K^+ \pi^- \pi^+, J/\psi K^+ K^- K^+$ [4], have been performed except for the B_c two-body decays. These kinds of decays are getting more and more attention, which is caused by the following reasons. First, these decays involve much more complicated QCD dynamics compared with the two-body decays because of entangled nonresonant and resonant contributions and significant final-state interactions. Second, many new resonance states are observed in the invariant mass distributions of the multihadron final states, which are difficult to understand in terms of a common hadron and called as exotic states. Last but not least, the direct CP violations for some of these decays can be analyzed in both two-body and multibody frameworks. In the multibody framework, the direct CP asymmetry may depend on the invariant mass distributions of the meson pair decaying from some internal resonances and be (strongly) affected by the finite widths of the resonances. Meanwhile, in the two-body framework with the resonance masses being fixed, the direct CP violation is just a number, which may be overestimated

*Corresponding author: zhangzhiqing@haut.edu.cn

or underestimated compared with the actual value. So it is important and necessary to research the B_c meson decays to the multihadron final states. In this work, one of our main purposes is to check the width effects of the resonance state K^* on the direct CP violations for the quasi-two-body decays $B_c \to K^* h \to K\pi h$ $(h = D, D_s, K, \pi, \eta, \eta')$ in the perturbative QCD (PQCD) approach. The other purpose is to understand the annihilation contributions under the three-body framework. As a feature of the PQCD approach, the annihilation-type Feynman diagrams are calculable, which are important for the decays occurring through the weak annihilation diagrams only.

In fact, in order to study the quasi-two-body $B_{(c)}$ meson decays, many approaches based on symmetry principles and factorization theorems have been proposed. Symmetry principles include the U-spin [5–7], isospin and flavor $SU(3)$ symmetry [8–11], and the factorization-assisted topological-diagram amplitude approach [12], etc. Factorization theorems include the QCD-improved factorization approach [13–17] and the PQCD approach [18–22]. It is argued that the factorization theorem of the quasi-two-body $B_{(c)}$ decays is approximately valid when the two particles move collinearly and the bachelor particle recoils back in the final states. According to this quasi-two-body-decay mechanism, the two-hadron distribution amplitudes (DAs) are introduced into the PQCD approach, where the strong dynamics between the two final hadrons in the resonant regions is included.

This paper is organized as follows. The framework of the PQCD approach for the quasi-two-body B_c decays is reviewed in Sec. II, where the kinematic variables for each meson are defined and the P-wave $K\pi$ pair distribution amplitudes up to twist 3 are parametrized. Then, the analytical formulas of decay amplitudes for each Feynman diagram and the total amplitudes for these decays are listed. In Sec. III, the numerical results and discussions are presented. The final section is devoted to our conclusions. Some details related functions are collected in the Appendix.

II. THE FRAMEWORK

In the framework of the PQCD approach for the quasi-two-body decays, the amplitude for the $B_c \to K^* h \to K\pi h$ decays can be written as [23,24]

$$\mathcal{A} = \Phi_{B_c} \otimes H \otimes \Phi_{K\pi}^{\text{P-wave}} \otimes \Phi_h, \tag{1}$$

where $\Phi_{B_c}(\Phi_h)$ denotes the DAs of the initial (final bachelor) meson, $\Phi_{K\pi}^{\text{P-wave}}$ represents the P-wave $K\pi$ pair DAs, and $\otimes$ denotes the convolution integrations over the parton momenta. Similar to the two-body decay case, the evolution of the hard kernel H for the b quark decay is calculable perturbatively and starts with the diagrams of single hard gluon exchange. The nonperturbative dynamics is absorbed into those DAs Φ_{B_c}, Φ_h, and $\Phi_{K\pi}^{\text{P-wave}}$.

In the rest frame of the B_c meson, we define the B_c meson momentum p_{B_c}, the $K(\pi)$ meson momentum $p_1(p_2)$, the K^* meson momentum $p = p_1 + p_2$, and the bachelor meson h momentum p_3 in light-cone coordinates as

$$p_{B_c} = \frac{m_{B_c}}{\sqrt{2}}(1, 1, \mathbf{0}_{\text{T}}), \qquad p = \frac{m_{B_c}}{\sqrt{2}}(1 - r^2, \eta, \mathbf{0}_{\text{T}}),$$
$$p_3 = \frac{m_{B_c}}{\sqrt{2}}(r^2, 1 - \eta, \mathbf{0}_{\text{T}}), \tag{2}$$

$$p_1 = \frac{m_{B_c}}{\sqrt{2}}(\zeta(1 - r^2), (1 - \zeta)\eta, \mathbf{p}_{1\text{T}}),$$
$$p_2 = \frac{m_{B_c}}{\sqrt{2}}((1 - \zeta)(1 - r^2), \zeta\eta, \mathbf{p}_{2\text{T}}), \tag{3}$$

where $\eta = w^2/[(1 - r^2)m_{B_c}^2]$ with the mass ratio $r = m_h/m_{B_c}$ and ζ is the momentum fraction for the kaon meson. The momenta of the light quarks in the B_c meson, the K^* meson, and the bachelor meson h are defined as k_B, k, and k_3, respectively:

$$k_B = (0, x_B p_B^-, \mathbf{k}_{B\text{T}}), \qquad k = (zp^+, 0, \mathbf{k}_{\text{T}}),$$
$$k_3 = (0, x_3 p_3^-, \mathbf{k}_{3\text{T}}), \tag{4}$$

where x_B, z, and x_3 are the corresponding momentum fractions.

A. Wave functions

In the course of the PQCD calculations, the necessary inputs contain the DAs, which are constructed via the nonlocal matrix elements. The B_c meson light-cone matrix element can be decomposed as

$$\int d^4 z e^{ik_B \cdot z} \langle 0|\bar{b}_\alpha(0) c_\beta(z)|B_c(p_{B_c})\rangle$$
$$= \frac{i}{\sqrt{2N_c}}[(\not{p}_{B_c} + M)\gamma_5 \phi_{B_c}(k_B)]_{\beta\alpha}, \tag{5}$$

where $N_c = 3$ is the color factor. Here, we consider only the contribution from the dominant Lorentz structure. In coordinate space, the distribution amplitude ϕ_{B_c} with an intrinsic b (the conjugate space coordinate to the transverse momentum k_T) dependence is adopted in a Gaussian form [25]:

$$\phi_{B_c}(x, b) = \frac{f_{B_c}}{2\sqrt{2N_c}} N_{B_c} x(1 - x) \exp\left[-\frac{(1 - x)m_c^2 + x m_b^2}{8\omega_b^2 x(1 - x)} - 2\omega_b^2 b^2 x(1 - x)\right], \tag{6}$$

where the decay constant $f_{B_c} = 0.489 \pm 0.005$ GeV is obtained in the lattice QCD [26] and the shape parameter $\omega_b = 1.0 \pm 0.1$ GeV is related to the factor N_{B_c} by the normalization $\int_0^1 \phi_{B_c}(x,0)dx = \frac{f_{B_c}}{2\sqrt{2N_c}}$. For the recent development on the transverse-momentum-dependent hadronic wave functions, one can find more in Refs. [27,28].

For the D meson, the light-cone distribution amplitudes (LCDAs) in the heavy quark limit can be written as [29,30]

$$\langle D(p_3)|q_\alpha(z)\bar{c}_\beta(0)|0\rangle = \frac{i}{\sqrt{2N_c}}\int_0^1 dx e^{ixp_3\cdot z}[\gamma_5(\not{p}_3 + m_D)\phi_D(x,b)]_{\alpha\beta}, \quad (7)$$

with the distribution amplitude $\phi_D(x,b)$:

$$\phi_D(x,b) = \frac{1}{2\sqrt{2N_c}} f_D 6x(1-x)[1 + C_D(1-2x)] \times \exp\left[\frac{-\omega^2 b^2}{2}\right], \quad (8)$$

where $C_D = 0.5 \pm 0.1$, $\omega = 0.1$ GeV, and $f_D = 211.9$ MeV. It is similar for the LCDAs of the D_s meson but with different parameters $C_{D_s} = 0.4 \pm 0.1$, $\omega = 0.2$ GeV, and $f_{D_s} = 249$ MeV, caused by a little SU(3) breaking effect [31]. As to the LCDAs for the light pseudoscalar mesons $\pi, K, \eta^{(\prime)}$ up to twist 3 can be found in our recent work [18].

The P-wave $K\pi$ pair distribution amplitudes are defined as [32]

$$\Phi_{K\pi}^{\text{P-wave}} = \frac{1}{\sqrt{2N_c}}\left[\not{p}\phi_0(z,\zeta,\omega^2) + \omega\phi_s(z,\zeta,\omega^2) + \frac{\not{n}_1\not{n}_2 - \not{n}_2\not{n}_1}{\omega(2\zeta-1)}\phi_t(z,\zeta,\omega^2)\right], \quad (9)$$

with the functions

$$\phi_0 = \frac{3F_{K\pi}(s)}{\sqrt{2N_c}} z(1-z)\left[1 + a_{1K^*}^{\parallel} 3(2z-1) + a_{2K^*}^{\parallel}\frac{3}{2}(5(2z-1)^2-1)\right]P_1(2\zeta-1),$$
$$\phi_s = \frac{3F_s(s)}{2\sqrt{2N_c}}(1-2z)P_1(2\zeta-1),$$
$$\phi_t = \frac{3F_t(s)}{2\sqrt{2N_c}}(2z-1)^2 P_1(2\zeta-1), \quad (10)$$

where the Legendre polynomial $P_1(2\zeta-1) = 2\zeta - 1$ and the Gegenbauer moments $a_{1K^*}^{\parallel} = 0.05 \pm 0.02$ and $a_{2K^*}^{\parallel} = 0.15 \pm 0.05$ [21]. It is well known that the relativistic Breit-Wigner (RBW) function is an appropriate model for the narrow resonances which can be well separated from any other resonant or nonresonant contributions with the same spin and is widely used in the experimental data analyses. Here, the timelike form factor $F_{K\pi}(s)$ with $s = \omega^2 = m^2(K\pi)$ via the RBW line shape is written as [33–35]

$$F_{K\pi}(s) = \frac{m_{K^*}^2}{m_{K^*}^2 - s - im_{K^*}\Gamma(s)}, \quad (11)$$

where the invariant mass-dependent width $\Gamma(s)$ is defined as

$$\Gamma(s) = \Gamma_{K^*}\frac{m_{K^*}}{\sqrt{s}}\left(\frac{|\overrightarrow{p_1}|}{|\overrightarrow{p_0}|}\right)^3 \frac{1 + (|\overrightarrow{p_0}|r_{\text{BW}})^2}{1 + (|\overrightarrow{p_1}|r_{\text{BW}})^2}. \quad (12)$$

Here, $|\vec{p}_1|$ is the magnitude of the momentum for the daughter meson K or π in the K^* meson rest frame defined in the next subsection, and $|\overrightarrow{p_0}|$ is the value of $|\overrightarrow{p_1}|$ at $s = m_{K^*}^2$. The barrier radius $r_{\text{BW}} = 4.0$ GeV^{-1} is taken as in Refs. [33–35].

B. Analytic formulas

For the quasi-two-body decays $B_c \to K^* D_{(s)} \to K\pi D_{(s)}$, the effective Hamiltonian relevant to the $b \to s(d)$ transition is given by [36]

$$H_{\text{eff}} = \frac{G_F}{\sqrt{2}}\left\{\sum_{q=u,c} V_{qb}V_{qs(d)}^*\left[C_1(\mu)O_1^{(q)}(\mu) + C_2(\mu)O_2^{(q)}(\mu)\right] - \sum_{i=3\sim10} V_{tb}V_{ts(d)}^* C_i(\mu)O_i(\mu)\right\} + \text{H.c.}, \quad (13)$$

where the Fermi coupling constant $G_F \simeq 1.166 \times 10^{-5}$ GeV^{-2} and $V_{qb}V_{qd(s)}^*$ and $V_{tb}V_{td(s)}^*$ are the products of the Cabibbo-Kobayashi-Maskawa (CKM) matrix elements. The scale μ separates the effective Hamiltonian into two distinct parts: the Wilson coefficients C_i and the local four-quark operators O_i. The local four-quark operators for $b \to d$ transition are written as

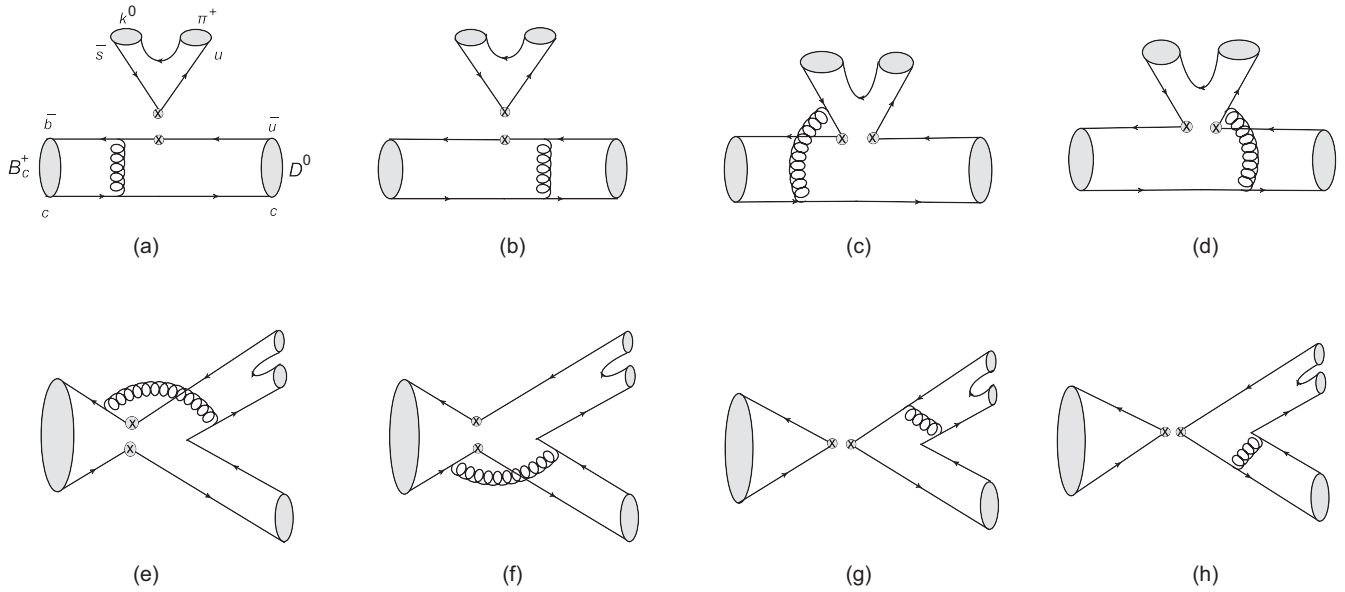

FIG. 1. The leading-order Feynman diagrams for the decay $B_c^+ \to K^{*+}D^0 \to K^0\pi^+D^0$.

$$
\begin{aligned}
O_1^{(q)} &= (\bar{d}_i q_j)_{V-A}(\bar{q}_j b_i)_{V-A}, & O_2^{(q)} &= (\bar{d}_i q_i)_{V-A}(\bar{q}_j b_j)_{V-A},\\
O_3 &= (\bar{d}_i b_i)_{V-A}\sum_q (\bar{q}_j q_j)_{V-A}, & O_4 &= (\bar{d}_i b_j)_{V-A}\sum_q (\bar{q}_j q_i)_{V-A},\\
O_5 &= (\bar{d}_i b_i)_{V-A}\sum_q (\bar{q}_j q_j)_{V+A}, & O_6 &= (\bar{d}_i b_j)_{V-A}\sum_q (\bar{q}_j q_i)_{V+A},\\
O_7 &= \frac{3}{2}(\bar{d}_i b_i)_{V-A}\sum_q e_q(\bar{q}_j q_j)_{V+A}, & O_8 &= \frac{3}{2}(\bar{d}_i b_j)_{V-A}\sum_q e_q(\bar{q}_j q_i)_{V+A},\\
O_9 &= \frac{3}{2}(\bar{d}_i b_i)_{V-A}\sum_q e_q(\bar{q}_j q_j)_{V-A}, & O_{10} &= \frac{3}{2}(\bar{d}_i b_j)_{V-A}\sum_q e_q(\bar{q}_j q_i)_{V-A},
\end{aligned}
\tag{14}
$$

where the color indices are i and j. Here, $V \pm A$ refer to the Lorentz structures $\gamma_\mu(1 \pm \gamma_5)$. The local four-quark operators for $b \to s$ transition can be obtained by replacing d with s in Eq. (14). While for the pure annihilation decays $B_c \to K^*\pi(K, \eta^{(\prime)}) \to K\pi\pi(K, \eta^{(\prime)})$, the related weak effective Hamiltonian is given as

$$
H_{\text{eff}} = \frac{G_F}{\sqrt{2}} V_{cb}V^*_{us(d)}\Big[C_1(\mu)O_1^{(q)}(\mu) + C_2(\mu)O_2^{(q)}(\mu)\Big], \tag{15}
$$

with the single tree operators

$$
O_1 = (\bar{d}_i u_j)_{V-A}(\bar{c}_j b_i)_{V-A}, \qquad O_2 = (\bar{d}_i u_i)_{V-A}(\bar{c}_j b_j)_{V-A} \quad (\text{for } b \to d \text{ transition}), \tag{16}
$$

$$
O_1 = (\bar{s}_i u_j)_{V-A}(\bar{c}_j b_i)_{V-A}, \qquad O_2 = (\bar{s}_i u_i)_{V-A}(\bar{c}_j b_j)_{V-A} \quad (\text{for } b \to s \text{ transition}). \tag{17}
$$

The typical Feynman diagrams at the leading order for the quasi-two-body decays $B_c \to K^*h \to K\pi h$ are shown in Fig. 1, where we take the decay $B_c^+ \to K^{*+}D^0 \to K^0\pi^+D^0$ as an example. We mark LL, LR, and SP to denote the contributions from $(V-A)(V-A)$, $(V-A)(V+A)$, and $(S-P)(S+P)$ operators,[1] respectively. The amplitudes from the factorizable emission diagrams Figs. 1(a) and 1(b) are given as

[1]It is noted that the $(S-P)(S+P)$ operators are obtained from $(V-A)(V+A)$ ones through the Fierz transformation to get the right color structure for factorization to work.

$$\mathcal{F}_e^{\mathrm{LL}} = 8\pi F_{K\pi} m_{B_c}^4 C_F \int_0^1 dx_B dx_3 \int_0^\infty b_1 b_3 db_1 db_3 \phi_B(x_B, b_1)\phi_D(x_3, b_3)\{[-\bar{\eta}[\eta(1-x_3)+x_3(1-2r)-2r_b] - rr_b(1+\eta)+r^2(x_3-2r_b)]\alpha_s(t_a)h(\alpha_e,\beta_a,b_1,b_3)\exp[-S_{ab}(t_a)]S_t(x_3) + [\bar{\eta}(2r+\eta x_B)-2rx_B(1+\eta)+r^2(x_B-1)]\times\alpha_s(t_b)h(\alpha_e,\beta_b,b_1,b_3)\exp[-S_{ab}(t_b)]S_t(x_B)\}, \tag{18}$$

$$\mathcal{F}_e^{\mathrm{LL}} = \mathcal{F}_e^{\mathrm{LR}}, \mathcal{F}_e^{\mathrm{SP}} = 0, \tag{19}$$

where $\bar{\eta} = 1-\eta$ and the mass ratio $r_b = m_b/m_{B_c}$. η and r have been defined under Eq. (3). The hard function $h(\alpha_e, \beta_a, b_1, b_3)$, the hard scales $t_{a,b}$, the Sudakov factor $\exp[-S_{ab}(t)]$, and the threshold resummation factor $S_t(x)$ are given in the Appendix. The amplitudes for the nonfactorizable emission diagrams Figs. 1(c) and 1(d) are written as

$$\mathcal{M}_e^{\mathrm{LL}} = 16\sqrt{\frac{2}{3}}\pi m_{B_c}^4 C_F \int_0^1 dx_B dz dx_3 \int_0^\infty b_1 b db_1 db \phi_B(x_B, b_1)\phi_D(x_3, b_1)\phi_0\{[r[(1+\eta)(x_B-1)+\bar{\eta}x_3+\eta z] + (1-\eta^2)(1-x_B-z)]\alpha_s(t_c)h(\beta_c,\alpha_e,b_1,b)\exp[-S_{cd}(t_c)] + [(r-\bar{\eta})(1-x_3)\bar{\eta} - r[(1+\eta)x_B-\eta z] + \bar{\eta}(2x_B-z)]\alpha_s(t_d)h(\beta_d,\alpha_e,b_1,b)\exp[-S_{cd}(t_d)]\}, \tag{20}$$

$$\mathcal{M}_e^{\mathrm{LR}} = 16\sqrt{\frac{2}{3}}\pi m_{B_c}^4 C_F\sqrt{\eta(1-r^2)} \int_0^1 dx_B dz dx_3 \int_0^\infty b_1 b db_1 db \phi_B(x_B, b_1)\phi_D(x_3, b_1)\phi_0\{[\bar{\eta}(1-x_B-z)(\phi^s+\phi^t) - r(\bar{\eta}x_3-z)(\phi^s-\phi^t)+2r(1-x_B-z)\phi^s]\alpha_s(t_c)h(\beta_c,\alpha_e,b_1,b)\exp[-S_{cd}(t_c)] + [r[\bar{\eta}(x_3-1)+z](\phi^s+\phi^t) + 2r(x_B-z)\phi^s + \bar{\eta}(x_B-z)(\phi^s-\phi^t)]\alpha_s(t_d)h(\beta_d,\alpha_e,b_1,b)\exp[-S_{cd}(t_d)]\}, \tag{21}$$

$$\mathcal{M}_e^{\mathrm{SP}} = 16\sqrt{\frac{2}{3}}\pi m_{B_c}^4 C_F \int_0^1 dx_B dz dx_3 \int_0^\infty b_1 b db_1 db \phi_B(x_B, b_1)\phi_D(x_3, b_1)\phi_0\{[(r-\bar{\eta})\bar{\eta}x_3 - r(1+\eta)(1-x_B) - rz\eta + \bar{\eta}[2(1-x_B)-z]]\alpha_s(t_c)h(\beta_c,\alpha_e,b_1,b)\exp[-S_{cd}(t_c)] + [r[\bar{\eta}(1-x_3)+\eta(z-x_B)-x_B] + (1-\eta^2)(x_B-z)]\alpha_s(t_d)h(\beta_d,\alpha_e,b_1,b)\exp[-S_{cd}(t_d)]\}. \tag{22}$$

It is noticed that the integration of b_3 has been performed using δ function $\delta(b_1-b_3)$, leaving only integration of b_1 and b. The amplitudes from the nonfactorizable annihilation diagrams Figs. 1(e) and 1(f) are listed as

$$\mathcal{M}_a^{\mathrm{LL}} = 16\sqrt{\frac{2}{3}}\pi m_{B_c}^4 C_F \int_0^1 dx_B dz dx_3 \int_0^\infty b_1 b_3 db_1 db_3 \phi_B(x_B, b_1)\phi_D(x_3, b_3)\phi_0\Big\{\Big[\bar{\eta}[(1+\eta)(1-x_B-z)-r_b]\phi^0 - r\sqrt{\eta(1-r^2)}[z(\phi^s+\phi^t)-\bar{\eta}x_3(\phi^s-\phi^t)]+2(2r_b+x_B-1)\phi^s\Big]\alpha_s(t_e)h(\beta_e,\alpha_a,b_1,b_3)\exp[-S_{ef}(t_e)] + \Big[\bar{\eta}[\bar{\eta}x_3-x_B(1+\eta)+r_c+\eta z]\phi^0 + r\sqrt{\eta(1-r^2)}[\bar{\eta}x_3(\phi^s+\phi^t)+z(\phi^s-\phi^t) + 2(2r_c-x_B)\phi^s]\Big]\alpha_s(t_f)h(\beta_f,\alpha_a,b_1,b_3)\exp[-S_{ef}(t_f)]\Big\}, \tag{23}$$

$$\mathcal{M}_a^{\mathrm{LR}} = 16\sqrt{\frac{2}{3}}\pi m_{B_c}^4 C_F \int_0^1 dx_B dz dx_3 \int_0^\infty b_1 b_3 db_1 db_3 \phi_B(x_B, b_1)\phi_D(x_3, b_3)\phi_0\Big\{[r[(1+\eta)(x_B-r_b-1)+\bar{\eta}x_3+\eta z]\phi^0 + \bar{\eta}\sqrt{\eta(1-r^2)}(1+r_b-x_B-z)(\phi^s+\phi^t)]\alpha_s(t_e)h(\beta_e,\alpha_a,b_1,b_3)\exp[-S_{ef}(t_e)] + r[(1+\eta)(x_B+r_c) - \bar{\eta}x_3-\eta z]\phi^0 - \bar{\eta}\sqrt{\eta(1-r^2)}(r_c+x_B-z)(\phi^s+\phi^t)\alpha_s(t_f)h(\beta_f,\alpha_a,b_1,b_3)\exp[-S_{ef}(t_f)]\Big\}. \tag{24}$$

The amplitudes from the factorizable annihilation diagrams Figs. 1(g) and 1(h) are listed as

$$\mathcal{F}_a^{\mathrm{LL}} = -8\pi f_{B_c} m_{B_c}^4 C_F \int_0^1 dz dx_3 \int_0^\infty b b_3 db db_3 \phi_D(x_3, b_3) \Big\{ \Big[\bar{\eta}(\bar{\eta} x_3 + \eta)\phi^0 + 2r\sqrt{\eta(1-r^2)}(1+\eta+\bar{\eta}x_3)\phi^s \Big] \alpha_s(t_g) h(\alpha_a, \beta_g, b, b_3) \exp[-S_{gh}(t_g)] S_t(x_3) + \Big[[2(1+\eta) r r_c - \bar{\eta} z + r^2(2x_2\bar{\eta} - 1)]\phi^0 - \sqrt{\eta(1-r^2)}[2rz(\phi^s + \phi^t) + (2r - r_c)\bar{\eta}(\phi^s - \phi^t)] \Big] \alpha_s(t_h) h(\alpha_a, \beta_h, b_3, b) \exp[-S_{gh}(t_h)] S_t(z) \Big\}, \tag{25}$$

$$\mathcal{F}_a^{\mathrm{SP}} = 16\pi f_{B_c} m_{B_c}^4 C_F \int_0^1 dz dx_3 \int_0^\infty b b_3 db db_3 \phi_D(x_3, b_3) \times \Big\{ [r(x_3\bar{\eta} + 2\eta)\phi^0 + 2\bar{\eta}\sqrt{\eta(1-r^2)}\,\phi^s] \alpha_s(t_g) h_e(\alpha_a, \beta_g, b, b_3) \exp[-S_{gh}(t_g)] S_t(x_3) + [[2rz\eta - \bar{\eta}(r_c - 2r)]\phi^0 + \sqrt{\eta(1-r^2)}[\bar{\eta} z(\phi^s - \phi^t) - 4r r_c \phi^s]] \times \alpha_s(t_h) h_e(\alpha_a, \beta_h, b_3, b) \exp[-S_{gh}(t_h)] S_t(z) \Big\}. \tag{26}$$

By combining the amplitudes from the different Feynman diagrams, the total decay amplitudes for the quasi-two-body decays $B_c \to K^* D_{(s)} \to K\pi D_{(s)}$ are given as

$$\mathcal{A}(B_c^+ \to K^{*+} D^0 \to K^0 \pi^+ D^0) = V_{us} V_{ub}^* [a_1 \mathcal{F}_e^{\mathrm{LL}} + C_1 \mathcal{M}_e^{\mathrm{LL}}] + V_{cs} V_{cb}^* [a_1 \mathcal{F}_a^{\mathrm{LL}} + C_1 \mathcal{M}_a^{\mathrm{LL}}] - V_{ts} V_{tb}^* \Big[(C_3 + C_9)(\mathcal{M}_e^{\mathrm{LL}} + \mathcal{M}_a^{\mathrm{LL}}) + (C_5 + C_7)(\mathcal{M}_e^{\mathrm{LR}} + \mathcal{M}_a^{\mathrm{LR}}) + \left(C_4 + \frac{1}{3}C_3 + C_{10} + \frac{1}{3}C_9\right)(\mathcal{F}_a^{\mathrm{LL}} + \mathcal{F}_e^{\mathrm{LL}}) + \left(C_6 + \frac{1}{3}C_5 + C_8 + \frac{1}{3}C_7\right)(\mathcal{F}_a^{\mathrm{SP}} + \mathcal{F}_e^{\mathrm{SP}}) \Big], \tag{27}$$

$$\mathcal{A}(B_c^+ \to K^{*0} D^+ \to K^+ \pi^- D^+) = V_{cs} V_{cb}^* [a_1 \mathcal{F}_a^{\mathrm{LL}} + C_1 \mathcal{M}_a^{\mathrm{LL}}] - V_{ts} V_{tb}^* \Big[\left(C_3 - \frac{1}{2}C_9\right)\mathcal{M}_e^{\mathrm{LL}} + (C_3 + C_9)\mathcal{M}_a^{\mathrm{LL}} + \left(C_5 - \frac{1}{2}C_7\right)\mathcal{M}_e^{\mathrm{LR}} + (C_5 + C_7)\mathcal{M}_a^{\mathrm{LR}} + \left(C_4 + \frac{1}{3}C_3 + C_{10} + \frac{1}{3}C_9\right)\mathcal{F}_a^{\mathrm{LL}} + \left(C_4 + \frac{1}{3}C_3 - \frac{1}{2}C_{10} - \frac{1}{6}C_9\right)\mathcal{F}_e^{\mathrm{LL}} + \left(C_6 + \frac{1}{3}C_5 - \frac{1}{2}C_8 - \frac{1}{6}C_7\right)\mathcal{F}_e^{\mathrm{SP}} + \left(C_6 + \frac{1}{3}C_5 + C_8 + \frac{1}{3}C_7\right)\mathcal{F}_a^{\mathrm{SP}} \Big], \tag{28}$$

$$\mathcal{A}(B_c^+ \to \bar{K}^{*0} D_s^+ \to K^- \pi^+ D_s^+) = V_{cd} V_{cb}^* [a_1 \mathcal{F}_a^{\mathrm{LL}} + C_1 \mathcal{M}_a^{\mathrm{LL}}] - V_{td} V_{tb}^* \Big[\left(C_3 - \frac{1}{2}C_9\right)\mathcal{M}_e^{\mathrm{LL}} + (C_3 + C_9)\mathcal{M}_a^{\mathrm{LL}} + \left(C_5 - \frac{1}{2}C_7\right)\mathcal{M}_e^{\mathrm{LR}} + (C_5 + C_7)\mathcal{M}_a^{\mathrm{LR}} + \left(C_4 + \frac{1}{3}C_3 + C_{10} + \frac{1}{3}C_9\right)\mathcal{F}_a^{\mathrm{LL}} + \left(C_4 + \frac{1}{3}C_3 - \frac{1}{2}C_{10} - \frac{1}{6}C_9\right)\mathcal{F}_e^{\mathrm{LL}} + \left(C_6 + \frac{1}{3}C_5 - \frac{1}{2}C_8 - \frac{1}{6}C_7\right)\mathcal{F}_e^{\mathrm{SP}} + \left(C_6 + \frac{1}{3}C_5 + C_8 + \frac{1}{3}C_7\right)\mathcal{F}_a^{\mathrm{SP}} \Big]. \tag{29}$$

Similarly, we can also obtain the total amplitudes for the pure annihilation decays $B_c \to K^* h \to K\pi h$ with $h = K, \pi, \eta^{(\prime)}$ as follows:

$$\mathcal{A}(B_c^+ \to \bar{K}^{*0} K^+ \to \bar{K}^0 \pi^0 K^+) = V_{ud} V_{cb}^* \left[a_1 \mathcal{F}_a^{\mathrm{LL}} + C_1 \mathcal{M}_a^{\mathrm{LL}} \right], \tag{30}$$

$$\mathcal{A}(B_c^+ \to K^{*+} \bar{K}^0 \to K^0 \pi^+ \bar{K}^0) = V_{ud} V_{cb}^* \left[a_1 \mathcal{F}_a^{\mathrm{LL}} + C_1 \mathcal{M}_a^{\mathrm{LL}} \right], \tag{31}$$

$$\mathcal{A}(B_c^+ \to K^{*+} \pi^0 \to K^0 \pi^+ \pi^0) = V_{us} V_{cb}^* \left[a_1 \mathcal{F}_a^{\mathrm{LL}} + C_1 \mathcal{M}_a^{\mathrm{LL}} \right], \tag{32}$$

$$\mathcal{A}(B_c^+ \to K^{*0} \pi^+ \to K^0 \pi^0 \pi^+) = \mathcal{A}(B_c^+ \to K^{*+} \pi^0 \to K^0 \pi^+ \pi^0), \tag{33}$$

$$\mathcal{A}(B_c^+ \to K^{*+} \eta \to K^0 \pi^+ \eta) = V_{us} V_{cb}^* \left[a_1 (\mathcal{F}_a^{LL,\eta_q} \cos\phi - \mathcal{F}_a^{LL,\eta_s} \sin\phi) + C_1 (\mathcal{M}_a^{LL,\eta_q} \cos\phi + \mathcal{F}_a^{LL,\eta_s} \sin\phi) \right], \tag{34}$$

$$\mathcal{A}(B_c^+ \to K^{*+} \eta' \to K^0 \pi^+ \eta') = V_{us} V_{cb}^* \left[a_1 (\mathcal{F}_a^{LL,\eta_q} \sin\phi + \mathcal{F}_a^{LL,\eta_s} \cos\phi) + C_1 (\mathcal{M}_a^{LL,\eta_q} \sin\phi + \mathcal{F}_a^{LL,\eta_s} \cos\phi) \right], \tag{35}$$

where the combinations of the Wilson coefficients $a_1 = C_2 + C_1/3$ and $a_2 = C_1 + C_2/3$ and the subscripts $\eta_{q,s}$ represent the two flavor states composing to the physical states η and η' as follows:

$$\begin{pmatrix} \eta \\ \eta' \end{pmatrix} = \begin{pmatrix} \cos\phi & -\sin\phi \\ \sin\phi & \cos\phi \end{pmatrix} \begin{pmatrix} \eta_q \\ \eta_s \end{pmatrix} \tag{36}$$

with $\phi = 39.3° \pm 1.0°$ [37].

Then the differential decay rate can be described as

$$\frac{d\mathcal{B}}{d\omega^2} = \tau_{B_c} \frac{|\vec{p}_1||\vec{p}_3|}{64\pi^3 m_B^3} |\mathcal{A}|^2, \tag{37}$$

where τ_{B_c} is the mean lifetime of B_c meson and the kinematic variables $|\vec{p}_1|$ and $|\vec{p}_3|$ denote the magnitudes of the K and the bachelor meson h momenta in the center-of-mass frame of the $K\pi$ pair:

$$|\vec{p}_1| = \frac{1}{2}\sqrt{\left[\left(m_K^2 - m_\pi^2\right)^2 - 2\left(m_K^2 + m_\pi^2\right)w^2 + w^4\right]/w^2},$$
$$|\vec{p}_3| = \frac{1}{2}\sqrt{\left[\left(m_{B_c}^2 - m_h^2\right)^2 - 2\left(m_{B_c}^2 + m_h^2\right)w^2 + w^4\right]/w^2}. \tag{38}$$

III. NUMERICAL RESULTS

The adopted input parameters in our numerical calculations are summarized as follows (the QCD scale, the masses, the decay constants, and the widths are in units of GeV, and the B_c meson lifetime is in units of picoseconds) [38]:

$$\begin{aligned} &\Lambda_{\mathrm{QCD}} = 0.25, \quad m_{B_c^+} = 6.274, \quad m_b = 4.8, \quad m_{K^\pm} = 0.494, \quad m_{K^0} = 0.498, \\ &m_{\pi^\pm} = 0.140, \quad m_{\pi^0} = 0.135, \quad m_{K^{*0}} = 0.89555, \quad m_{K^{*\pm}} = 0.89176, \\ &f_{K^*} = 0.217, \quad \Gamma_{K^{*0}} = 0.0462, \quad \Gamma_{K^{*\pm}} = 0.0514, \quad \tau_{B_c} = 0.51. \end{aligned} \tag{39}$$

As to the CKM matrix elements, we employ the Wolfenstein parametrization with the inputs [38]

$$\begin{aligned} &\lambda = 0.22500 \pm 0.00067, \quad A = 0.826^{+0.018}_{-0.015}, \\ &\bar{\rho} = 0.159 \pm 0.010, \quad \bar{\eta} = 0.348 \pm 0.010. \end{aligned} \tag{40}$$

By using the differential branching ratio in Eq. (37) and the squared amplitudes in Eqs. (27)–(35), integrating over the full $K\pi$ invariant mass region $(m_K + m_\pi) \le \omega \le (M_{B_c} - m_h)$ with $h = D_{(s)}, K, \pi, \eta^{(\prime)}$, we obtain the branching ratios for these quasi-two-body decays as

$$\mathrm{Br}(B_c^+ \to K^{*+} D^0 \to K^0 \pi^+ D^0) = (8.74^{+1.30+0.04+0.00+1.61}_{-1.43-0.03-0.01-1.03}) \times 10^{-7}, \tag{41}$$

$$\mathrm{Br}(B_c^+ \to K^{*0} D^+ \to K^+ \pi^- D^+) = (14.0^{+0.73+0.02+0.00+2.20}_{-3.06-0.14-0.14-2.35}) \times 10^{-7}, \tag{42}$$

$$\mathrm{Br}(B_c^+ \to \bar{K}^{*0} D_s^+ \to K^- \pi^+ D_s^+) = (1.17^{+0.19+0.03+0.05+0.00}_{-0.22-0.00-0.00-0.44}) \times 10^{-7}, \tag{43}$$

$$\mathrm{Br}(B_c^+ \to \bar{K}^{*0}K^+ \to \bar{K}^0\pi^0K^+) = (3.32^{+0.01+0.14+0.01+1.37}_{-0.00-0.13-0.00-0.00}) \times 10^{-7}, \quad (44)$$

$$\mathrm{Br}(B_c^+ \to K^{*+}\overline{K^0} \to K^0\pi^+\overline{K^0}) = (1.30^{+0.15+0.05+0.15+0.00}_{-0.01-0.09-0.06-0.37}) \times 10^{-7}, \quad (45)$$

$$\mathrm{Br}(B_c^+ \to K^{*0}\pi^+ \to K^0\pi^0\pi^+) = (0.74^{+0.00+0.01+0.00+1.09}_{-0.00-0.01-0.00-0.24}) \times 10^{-8}, \quad (46)$$

$$\mathrm{Br}(B_c^+ \to K^{*+}\pi^0 \to K^0\pi^+\pi^0) = (0.74^{+0.00+0.01+0.01+0.81}_{-0.01-0.01-0.01-0.41}) \times 10^{-8}, \quad (47)$$

$$\mathrm{Br}(B_c^+ \to K^{*+}\eta \to K^0\pi^+\eta) = (0.50^{+0.01+0.03+0.09+0.35}_{-0.00-0.03-0.08-0.13}) \times 10^{-8}, \quad (48)$$

$$\mathrm{Br}(B_c^+ \to K^{*+}\eta' \to K^0\pi^+\eta') = (1.58^{+0.00+0.00+0.04+0.00}_{-0.01-0.02-0.09-1.31}) \times 10^{-8}, \quad (49)$$

where the first error is from the B_c meson shape parameter uncertainty $\omega_{B_c} = 1.0 \pm 0.1$ GeV, the following two errors come from the Gegenbauer coefficients in the $K\pi$ pair distribution amplitudes $a^{\parallel}_{1K^*} = 0.05 \pm 0.02$ and $a^{\parallel}_{2K^*} = 0.15 \pm 0.05$, and the last one is induced by varying the hard scale t from $0.75t$ to $1.25t$ (without changing $1/b_i$) and QCD scale $\Lambda_{\mathrm{QCD}} = 0.25 \pm 0.05$ GeV, which characterize the next-to-leading-order effect in the PQCD approach. One can find that the errors induced by $a^{\parallel}_{1K^*}$ and $a^{\parallel}_{2K^*}$ are from a few percent to 15% for most of these considered decays. For the pure annihilation decay modes, the error stemming from the uncertainty of the B_c meson shape parameter ω_{B_c} is small. It can be roughly understood from the analytical formulas Eqs. (30)–(35). Because the Wilson coefficient $a_1 = C_2 + C_1/3$ is larger than C_1, the main contribution comes from the factorizable annihilation amplitude $\mathcal{F}_a^{\mathrm{LL}}$, where the terms about ω_{B_c} are not involved. The situation is a little different with the decay $B_c^+ \to K^{*+}D^0 \to K^0\pi^+D^0$, where the error induced by ω_{B_c} can reach 16%. By comparison, the branching ratios of these pure annihilation decays are more sensitive to the variation of the hard scale t and the QCD scale Λ_{QCD}. It means that these decays might be sensitive to the higher-order corrections. The errors arise from the uncertainties of the parameters; for instance, the Wolfenstein parameters, the pole mass of m_{K^*}, and the width Γ_{K^*} are very small and have been neglected. Furthermore, the branching ratios for the decays involving the η, η' mesons are not sensitive to the variation of the $\eta - \eta'$ mixing angle $(\phi = 39.3 \pm 1.0)°$, and the corresponding uncertainties from the branching ratios are less than 1%.

If we assume the isospin conservation for the strong decays $K^* \to K\pi$, namely

$$\frac{\Gamma(K^{*0} \to K^+\pi^-)}{\Gamma(K^{*0} \to K\pi)} = 2/3, \quad \frac{\Gamma(K^{*0} \to K^0\pi^0)}{\Gamma(K^{*0} \to K\pi)} = 1/3,$$
$$\frac{\Gamma(K^{*+} \to K^0\pi^+)}{\Gamma(K^{*+} \to K\pi)} = 2/3, \quad \frac{\Gamma(K^{*+} \to K^+\pi^0)}{\Gamma(K^{*+} \to K\pi)} = 1/3, \quad (50)$$

under the narrow width approximation relation, the branching ratio of each quasi-two-body decay can be related with that of the corresponding two-body decay using a simple formula. Take the decay $B_c^+ \to K^{*+}D^0 \to K^0\pi^+D^0$ as an example, the formula can be expressed as

TABLE I. The CP averaged branching ratios for the two-body decays $B_c^+ \to K^*h$ with $h = D_{(s)}, K, \pi, \eta^{(\prime)}$. The errors are the same as those given in Eqs. (41)–(49).

Decay modes	This work	Two-body framework [40,41]	RCQM [42]
$B_c^+ \to K^{*+}D^0$	$(1.31^{+0.20+0.01+0.00+0.24}_{-0.21-0.01-0.00-0.16}) \times 10^{-6}$	$(2.59^{+0.27+0.09+0.15}_{-0.30-0.08-0.08}) \times 10^{-6}$	3.47×10^{-6}
$B_c^+ \to K^{*0}D^+$	$(2.10^{+0.11+0.00+0.00+0.33}_{-0.46-0.02-0.02-0.35}) \times 10^{-6}$	$(1.91^{+0.33+0.01+0.07}_{-0.25-0.00-0.07}) \times 10^{-6}$	2.88×10^{-6}
$B_c^+ \to \bar{K}^{*0}D_s^+$	$(1.76^{+0.28+0.04+0.07+0.00}_{-0.33-0.00-0.00-0.66}) \times 10^{-7}$	$(1.4^{+0.2+0.0+0.1}_{-0.2-0.1-0.1}) \times 10^{-7}$	1.0×10^{-7}
$B_c^+ \to \bar{K}^{*0}K^+$	$(9.97^{+0.03+0.42+0.04+4.10}_{-0.00-0.39-0.00-0.00}) \times 10^{-7}$	$(10.0^{+0.5+1.7+0.0}_{-0.6-3.3-0.2}) \times 10^{-7}$	⋯
$B_c^+ \to K^{*+}\bar{K}^0$	$(1.95^{+0.21+0.07+0.22+0.00}_{-0.01-0.14-0.09-0.55}) \times 10^{-7}$	$(1.8^{+0.7+4.1+0.1}_{-0.1-2.1-0.0}) \times 10^{-7}$	⋯
$B_c^+ \to K^{*0}\pi^+$	$(2.23^{+0.00+0.03+0.00+3.27}_{-0.00-0.02-0.01-0.73}) \times 10^{-8}$	$(3.3^{+0.7+0.4+0.2}_{-0.2-0.4-0.1}) \times 10^{-8}$	⋯
$B_c^+ \to K^{*+}\pi^0$	$(1.11^{+0.00+0.01+0.02+1.21}_{-0.01-0.02-0.02-0.62}) \times 10^{-8}$	$(1.6^{+0.4+0.3+0.1}_{-0.1-0.1-0.0}) \times 10^{-8}$	
$B_c^+ \to K^{*+}\eta$	$(0.75^{+0.01+0.04+0.13+0.52}_{-0.00-0.04-0.12-0.20}) \times 10^{-8}$	$(0.9^{+0.1+0.6+0.0}_{-0.0-0.2-0.0}) \times 10^{-8}$	⋯
$B_c^+ \to K^{*+}\eta'$	$(2.37^{+0.00+0.00+0.06+0.00}_{-0.02-0.03-0.14-1.97}) \times 10^{-8}$	$(3.8^{+1.1+1.0+0.0}_{-1.1-0.6-0.0}) \times 10^{-8}$	⋯

$$\mathrm{Br}(B_c^+ \to K^{*+} D^0 \to K^0 \pi^+ D^0) = \mathrm{Br}(B_c^+ \to K^{*+} D^0) \cdot \mathrm{Br}(K^{*+} \to K^0 \pi^+). \quad (51)$$

Then we can obtain the branching ratios of the relevant two-body decays from those of the considered quasi-two-body decays, which are listed in Table I. In these considered decays, $B_c^+ \to K^{*+} D^0$ and $B_c^+ \to K^{*0} D^+$ have the largest branching ratios which can reach up to 10^{-6} and are possible measured by the future High-Energy LHC (HE-LHC) and High-Luminosity LHC (HL-LHC) experiments [39]. From our calculations, we find that, in these decays with $D_{(s)}$ meson involved, the penguin amplitudes are dominated. Although the values of the CKM matrix elements $V_{cb}V_{cs(d)}$ and $V_{tb}V_{ts(d)}$ are close to each other, the tree contributions associated with $V_{cb}V_{cs(d)}$ are from the annihilation-type amplitudes and very tiny. For example, such contributions are only about 2.9(1.1)% of the total branching ratio for the decay $B_c^+ \to K^{*0} D^+ (B_c^+ \to \bar{K}^{*0} D_s^+)$. There are some differences in the decay $B_c^+ \to K^{*+} D^0$, which receives two kinds of tree contributions: One is associated with the CKM matrix elements $V_{ub}^* V_{us}$, and the other is associated with the CKM elements $V_{cb}^* V_{cs}$. Although $V_{ub}^* V_{us}$ is smaller than $V_{cb}^* V_{cs} (\frac{V_{ub}^* V_{us}}{V_{cb}^* V_{cs}} = 0.0215)$, the former is connected with the (non)factorizable emission amplitude $\mathcal{F}_e^{\mathrm{LL}} (\mathcal{M}_e^{\mathrm{LL}})$, and the latter is connected with the (non) factorizable annihilation amplitude $\mathcal{F}_a^{\mathrm{LL}} (\mathcal{M}_a^{\mathrm{LL}})$ shown in Eq. (27). It is interesting that the differences from the amplitudes are huge enough to compensate the differences from the CKM elements. In fact, the proportions of these three kinds of contributions being connected with $V_{tb}^* V_{ts}$, $V_{ub}^* V_{us}$, and $V_{cb}^* V_{cs}$ in the total branching ratios are 1:0.24:0.06. So the tree contributions coming from CKM matrix elements $V_{ub}^* V_{us}$ are more important than those from $V_{cb}^* V_{cs}$ in the decay $B_c^+ \to K^{*+} D^0$. Although these tree contributions are not much helpful to increase the branching ratio, they are important to the direct CP violation of the decay $B_c^+ \to K^{*+} D^0$. Because of the absence of the tree contribution from the factorizable and nonfactorizable emission amplitudes in the decays $B_c^+ \to K^{*0} D^+$ and $B_c^+ \to \bar{K}^{*0} D_s^+$, the direct CP asymmetries in these two decays may be smaller. We will make a detailed discussion on this topic in the latter. As to the decay $B_c^+ \to \bar{K}^{*0} D_s^+$, its analytical formulas for the tree (penguin) amplitudes are almost the same as those for the decay $B_c^+ \to K^{*0} D^+$ (the differences are from the wave functions of D and D_s), while the value of the corresponding CKM elements $V_{cd}(V_{td})$ is only about 0.2 times that of $V_{cs}(V_{ts})$. So the branching ratio of the decay $B_c^+ \to \bar{K}^{*0} D_s^+$ is much smaller and only about the order of 10^{-7}. Compared with the branching ratios obtained in the previous PQCD calculations under the two-body framework [40,41], one can find that three-body and two-body calculations about these decays are consistent with each other; it supports the PQCD approach to exclusive hadronic B_c meson decays. For the decay $B_c^+ \to K^{*+} D^0$, its branching ratio is smaller than the result given by the relativistic constituent quark model (RCQM) [42] but is much larger than 0.68×10^{-7} predicted by the light front quark model (LFQM) [43] and 1.36×10^{-7} given by the Salpeter method [44]. This is because that the contributions from annihilation diagrams and penguin diagrams are missed in the LFQM and Salpeter method, so the decays dominated by the annihilation and penguin contributions might not be well predicted by these approaches. It is no surprise that $\mathrm{Br}(B_c^+ \to K^{*0} D^+) = 1.59 \times 10^{-7}$ and $\mathrm{Br}(B_c^+ \to \bar{K}^{*0} D_s^+) = 2.09 \times 10^{-8}$ given by the Salpeter method are almost one order of magnitude smaller than the PQCD predictions. It is meaningful to clarify these divergences in the future LHCb experiments. For the pure annihilation decays $B_c \to K^* h$ with h representing a light pseudoscalar meson K, π, or $\eta^{(\prime)}$, there are two decay modes; one is strange decay ($\Delta S = 1$) corresponding to the smaller CKM matrix element $V_{us} \sim 0.22$, which refers to $B_c^+ \to K^{*0}\pi^+, K^{*+}\pi^0, K^{*+}\eta^{(\prime)}$, and the other is nonstrange decay ($\Delta S = 0$) corresponding to the larger CKM matrix element $V_{us} \sim 1$, which refers to $B_c^+ \to \bar{K}^{*0} K^+, K^{*+}\bar{K}^0$. One can find that the branching ratios for the $\Delta S = 0$ channels are much larger than those for the $\Delta S = 1$ decays. For these two $\Delta S = 0$ processes, the decay $B_c^+ \to \bar{K}^{*0} K^+$ has the larger branching ratio, which is near 10^{-6} and possibly observed by the future LHCb experiments. It is interesting that this result is consistent with the estimation from the SU(3) flavor symmetry [45]. Although both of the decays $B_c^+ \to \bar{K}^{*0} K^+$ and $B_c^+ \to K^{*+}\bar{K}^0$ belong to the same decay mode, there exists a large gap between their branching ratios. It is very different for the case of $\mathrm{Br}(B_u^+ \to \bar{K}^{*0} K^+)$ and $\mathrm{Br}(B_u^+ \to K^{*+}\bar{K}^0)$, which are close to each other predicted by many theoretical approaches, such as the PQCD approach [46], the QCD factorization approach [47], and the soft-collinear effective theory [48]. Such abnormality shows significant difference for the annihilation amplitudes between the B (heavy-light system) and B_c (heavy-heavy system) decays. If this point can be clarified by the experiments, it will be helpful to further improve our understanding of the annihilation contributions.

The decay amplitudes of the quasi-two-body decays depend on the $K\pi$ invariant mass, which are different from the fixed kinematics in the two-body decays. So we can plot the differential distribution of the branching ratios shown in Fig. 2, where we take the decays with $D_{(s)}$ involved as examples. One can see that the differential branching ratios for these three decays exhibit peaks at the K^* meson mass. The main portion of the branching ratios lies in the region around the pole mass of the K^* resonance as expected. For example, the branching ratio obtained by integrating over ω in the range $m_{K^*} - \Gamma_{K^*}$ to $m_{K^*} + \Gamma_{K^*}$ is about 70% of the total decay rate for the channel $B_c^+ \to K^{*+} D^0 \to K^0 \pi^+ D^0$. Although we plot the differential branching ratios versus the

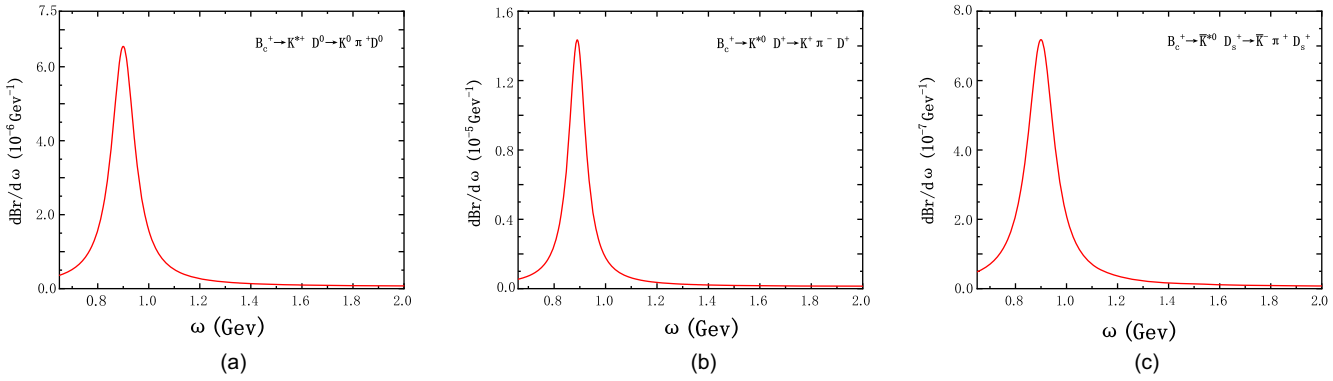

FIG. 2. The predicted $B_c \to K^* D_{(s)} \to K\pi D_{(s)}$ decay spectra in the $K\pi$ invariant mass.

invariant mass ω in the range $m_K + m_\pi$ to 2 GeV, the contributions from the energy region $\omega > 1.2$ GeV can be neglected safely.

Now we turn to the evaluations of the CP violation for the decays with $D_{(s)}$ meson involved. The direct CP violations induced from the interference between the tree and penguin amplitudes can be defined as

$$A_{CP} = \frac{\Gamma(B_c^- \to \bar{f}) - \Gamma(B_c^+ \to f)}{\Gamma(B_c^- \to \bar{f}) + \Gamma(B_c^+ \to f)}, \tag{52}$$

where $\bar{f}$ is the CP conjugated final state of f. The numerical results for these direct CP asymmetries are given as

$$A_{CP}(B_c^+ \to K^{*+} D^0 \to K^0 \pi^+ D^0) = (-14.6^{+2.7+0.4+0.0+8.8}_{-1.0-0.5-0.1-0.0}) \times 10^{-2}, \tag{53}$$

$$A_{CP}(B_c^+ \to K^{*0} D^+ \to K^+ \pi^- D^+) = (-0.14^{+0.02+0.01+0.02+0.13}_{-0.00-0.01-0.02-0.00}) \times 10^{-2}, \tag{54}$$

$$A_{CP}(B_c^+ \to \bar{K}^{*0} D_s^+ \to K^- \pi^+ D_s^+) = (1.07^{+0.22+0.13+0.18+0.00}_{-0.42-0.24-0.09-7.61}) \times 10^{-2}, \tag{55}$$

where the errors are the same with those given in Eqs. (41)–(49). Unlike the branching ratio, the direct CP asymmetry is not sensitive to the parameters in DAs but suffers from large uncertainties due to the hard scale t and the QCD scale $\Lambda_{\rm QCD}$, which can be reduced by including the high-order corrections. From the numerical results, we find the following points.

(1) Under the three-body framework calculations, there do not exist so large direct CP violations as more than 60% in magnitude predicted by the previous PQCD calculations [40] for the decays $B_c \to K^{*+} D^0, \bar{K}^{*0} D_s^+$. Our predictions are more comparable with those given by the Salpeter method and the RCQM shown in Table II. These results can be clarified by the future LHCb experiments.

(2) Compared with the channel $B_c^+ \to K^{*0} D^+ \to K^+ \pi^- D^+$, the decay $B_c^+ \to K^{*+} D^0 \to K^0 \pi^+ D^0$ receives more tree amplitude contributions, which come from not only the emission diagrams, but also the annihilation diagrams. Although the emission factorizable amplitude $F_e^{\rm LL}$ is suppressed by the CKM matrix elements $V_{us} V_{ub}^*$, it still provides strong interference with the penguin amplitudes because of the large Wilson coefficient $a_1 = C_2 + C_1/3$. So there exists more significant direct CP violation in the decay $B_c^+ \to K^{*+} D^0 \to K^0 \pi^+ D^0$ as we expected.

(3) As to the decay $B_c^+ \to K^{*0} D^+ \to K^+ \pi^- D^+$, although the CKM matrix element products $V_{cs} V_{tb}^*$ and $V_{ts} V_{tb}^*$ associated with the tree and penguin amplitudes, respectively, are almost equal to each other, the tree contributions from the

TABLE II. The direct CP violation ($\times 10^{-2}$) of the decays $B_c^+ \to K^{*+} D^0$, $B_c^+ \to K^{*0} D^+$, and $B_c^+ \to \bar{K}^{*0} D_s^+$, where the various errors have been added in quadrature. By comparison, we also give the results from the PQCD approach in the two-body framework [40], the Salpeter method [44], and the RCQM [42].

Decay modes	This work	PQCD (two-body framework) [40]	Salpeter method [44]	RCQM [42]
$B_c^+ \to K^{*+} D^0$	$-14.6^{+9.2}_{-1.1}$	$-66.2^{+15.2}_{-6.5}$	−25.5	−6.22
$B_c^+ \to K^{*0} D^+$	$-0.14^{+0.13}_{-0.02}$	$3.5^{+0.7}_{-0.9}$	−0.53	−0.822
$B_c^+ \to \bar{K}^{*0} D_s^+$	$1.07^{+0.31}_{-7.63}$	$61.0^{+7.9}_{-14.7}$	9.04	13.3

annihilation-type amplitudes are very small and about 2 orders lower than the penguin contributions. So the interference between these two kinds of contributions is weak, which induces much smaller CP violation.

(4) The amplitudes of the decay $B_c^+ \to \bar{K}^{*0} D_s^+ \to K^- \pi^+ D_s^+$ can be obtained from those of the channel $B_c^+ \to K^{*0} D^+ \to K^+ \pi^- D^+$ by replacing $D^+(V_{ts}, V_{cs})$ with $D_s^+(V_{td}, V_{cd})$. The total decay amplitudes for these two decays can be rewritten as

$$\mathcal{A} = V_{cb}^* V_{cq} T - V_{tb}^* V_{tq} P = V_{cb}^* V_{cq} T \left[1 + z e^{i(\alpha+\delta)}\right], \tag{56}$$

where T and P are the tree and penguin amplitudes, respectively, and α and δ are the weak and strong phases, respectively. The parameters z and α are defined as

$$z = \left| \frac{V_{tb}^* V_{tq}}{V_{cb}^* V_{cq}} \frac{P}{T} \right|, \qquad \alpha = \arg\left[-\frac{V_{tb}^* V_{tq}}{V_{cb}^* V_{cq}} \right], \tag{57}$$

with $q = d(s)$ for the decay $B_c^+ \to \bar{K}^{*0} D_s^+ \to K^- \pi^+ D_s^+ (B_c^+ \to K^{*0} D^+ \to K^+ \pi^- D^+)$. Then the direct CP asymmetries are

$$A_{CP} = \frac{2z \sin\alpha \sin\delta}{z^2 + 1 + 2\cos\alpha \cos\delta}. \tag{58}$$

As the weak phases are measured as $\arg[-\frac{V_{tb}^* V_{td}}{V_{cb}^* V_{cd}}] \sim -0.40$ and $\arg[-\frac{V_{tb}^* V_{ts}}{V_{cb}^* V_{cs}}] \sim 0.02$ [38], their corresponding sine values are about -0.39 and 0.02, respectively. So one can find that the size of $A_{CP}(B_c \to \bar{K}^{*0} D_s^+)$ is larger than that of $A_{CP}(B_c^+ \to K^{*0} D^+)$ mainly because of the larger weak phase in the former. They have opposite signs due to the differences from the weak phases.

Last, we plot the differential distributions of the direct CP violations for the decays $B_c^+ \to K^{*+} D^0 \to K^0 \pi^+ D^0$, $B_c^+ \to K^{*0} D^+ \to K^+ \pi^- D^+$, and $B_c \to \bar{K}^{*0} D_s^+ \to K^- \pi^+ D_s^+$ shown in Fig. 3. The measured CP violation is just a number in the two-body framework, where the K^* resonance mass is fixed to m_{K^*} during the calculations, while the direct CP violation in the three-body framework is dependent on the $K\pi$ invariant mass ω. So the total direct CP asymmetry is the integration of the corresponding differential distribution over ω. The integrated direct CP asymmetry for the quasibody decays may be very different with that obtained in the two-body framework; that is to say, the latter may be overestimated or underestimated compared with the actual value. In view of this point, the three-body framework should be more appropriate for studying the quasi-two-body decays. Here, we also find that the differential distribution curve for $A_{CP}(B_c \to \bar{K}^{*0} D_s^+ \to K^- \pi^+ D_s^+)$ lies in the positive value region, which is contrary to the cases of $A_{CP}(B_c \to K^{*+} D^0 \to K^0 \pi^+ D^0)$ and $A_{CP}(B_c^+ \to K^{*0} D^+ \to K^+ \pi^- D^+)$. It is mainly because of the differences from the weak phases.

IV. SUMMARY

In this paper, we studied the quasi-two-body decays $B_c \to K^* h \to K\pi h$ with $h = D, D_s, K, \pi, \eta, \eta'$ by using the PQCD approach. Under the quasi-two-body-decay mechanism, the $K\pi$ pair DAs were introduced, which include the final-state interactions between the $K\pi$ pair in the resonant region. Both the resonant and nonresonant contributions are described by the timelike form factors $F_{K\pi}(s)$, which are parametrized by using the relativistic Breit-Wigner formula for the P-wave resonance K^*. Under the narrow width approximation relation and the isospin conservation, the branching ratios for the two-body decays $B_c^+ \to K^{*+} h$ can be related with those of the considered quasi-two-body decays, so it provides us a new way to study these quasi-two-body B_c decays in the three-body framework. We found that the branching ratios are consistent with those calculated under the two-body framework. It supports the PQCD approach to exclusive hadronic B_c meson decays.

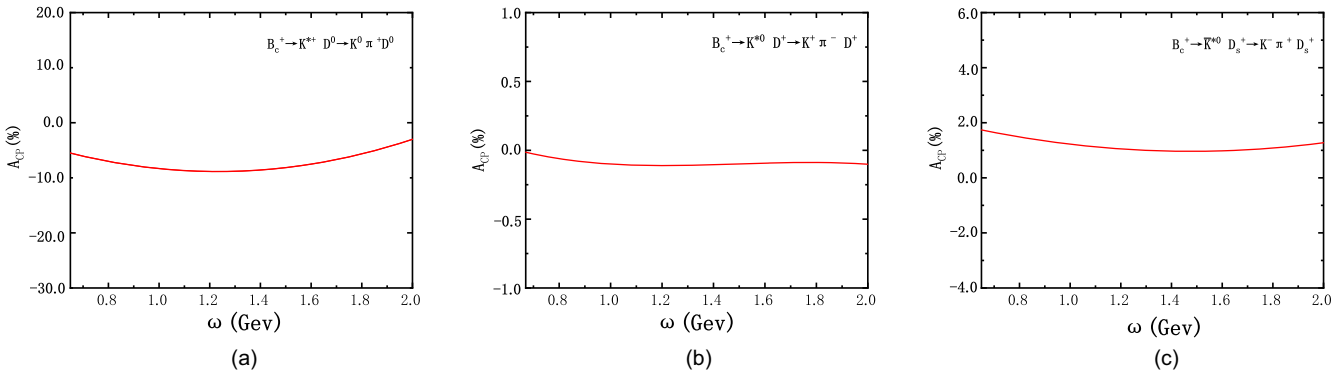

FIG. 3. The differential distributions of A_{CP} in ω for the decays $B_c^+ \to K^{*+} D^0 \to K^0 \pi^+ D^0$, $B_c^+ \to K^{*0} D^+ \to K^+ \pi^- D^+$, and $B_c^+ \to \bar{K}^{*0} D_s^+ \to K^- \pi^+ D_s^+$.

For the direct CP violation, there exist significant differences between the three-body and two-body frameworks. Under the two-body framework with the kinematics fixed, the direct CP violation A_{CP} is just a number, while under the three-body framework the direct CP asymmetry is a differential distribution, which depends on the $K\pi$ invariant mass ω. It is more convenient to compare with the Dalitz-plot analysis of A_{CP} provided by experiments. The A_{CP} calculated in the two-body framework corresponds to that in the three-body framework with the $K\pi$ invariant mass ω being fixed to K^* pole mass. In general, the integration of the A_{CP} differential distribution over the invariant mass ω under the three-body framework is different from that obtained under the two-body framework; the latter is usually overestimated or underestimated. Compared with the direct CP violations for the decays $B_c \to K^* D_{(s)}$ obtained in these two frameworks under the PQCD approach, the results from the three-body framework are moderated by the finite width of the K^* resonance and become comparable with those calculated within other theoretical approaches, such as the Salpeter method and the RCQM. This indicates that it is more appropriate to study the quasi-two-body B_c meson decays in the three-body framework than in the two-body framework. These results can be tested by future experiments.

We also researched the annihilation amplitude contributions to the pure annihilation decay modes $B_c \to K^* h \to K\pi h$ with $h = K, \pi, \eta, \eta'$ in the three-body framework and found there exist significant differences in the annihilation amplitudes between the B (heavy-light system) and B_c (heavy-heavy system) decays through comparing the branching ratios of the decays $B^+ \to \bar{K}^{*0} K^+, K^{*+} \bar{K}^0$ and $B_c^+ \to \bar{K}^{*0} K^+, K^{*+} \bar{K}^0$. If such a point can be clarified by future experiments, it will be helpful to further improve our understanding about the annihilation contributions. Furthermore, among these considered pure annihilation decays, the channel $B_c^+ \to K^{*+} \bar{K}^0$ has the largest branching ratio, which is near 10^{-6}. It is possibly observed by the LHCb experiments.

ACKNOWLEDGMENTS

We thank Professor Hsiang-nan Li for valuable discussions. This work is partly supported by the National Natural Science Foundation of China under Grant No. 11347030, by the Program of Science and Technology Innovation Talents in Universities of Henan Province 14HASTIT037, and Natural Science Foundation of Henan Province under Grant No. 232300420116.

APPENDIX: SOME RELEVANT FUNCTIONS

The explicit expressions of the hard functions h_i with $i = (a, \ldots, h)$ are obtained from the Fourier transform of the hard kernels and given as

$$
\begin{aligned}
h_i(\alpha, \beta, b_1, b_2) &= h_1(\beta, b_2) \times h_2(\alpha, b_1, b_2), \\
h_1(\beta, b_2) &= \begin{cases} K_0(\sqrt{\beta} b_2), & \beta > 0; \\ K_0\left(i\sqrt{-\beta} b_2\right), & \beta < 0; \end{cases} \\
h_2(\alpha, b_1, b_2) &= \begin{cases} \theta(b_2 - b_1) I_0(\sqrt{\alpha} b_1) K_0(\sqrt{\alpha} b_2) + (b_1 \leftrightarrow b_2), & \alpha > 0; \\ \theta(b_2 - b_1) I_0(\sqrt{-\alpha} b_1) K_0(i\sqrt{-\alpha} b_2) + (b_1 \leftrightarrow b_2), & \alpha < 0; \end{cases}
\end{aligned} \tag{A1}
$$

where K_0 and I_0 are modified Bessel functions with $K(ix) = \frac{\pi}{2}(-N_0(x) + iJ_0(x))$ and J_0 is a Bessel function. The hard scales t_i are chosen as the maximum of the virtuality of the internal momentum transition in the hard amplitudes and listed as follows:

$$
\begin{aligned}
t_a &= \max\left\{m_{B_c}\sqrt{|\alpha_a|}, m_{B_c}\sqrt{|\beta_a|}, 1/b_3, 1/b_1\right\}, & t_b &= \max\left\{m_{B_c}\sqrt{|\alpha_b|}, m_{B_c}\sqrt{|\beta_b|}, 1/b_1, 1/b_3\right\}, \\
t_c &= \max\left\{m_{B_c}\sqrt{|\alpha_c|}, m_{B_c}\sqrt{|\beta_c|}, 1/b_1, 1/b\right\}, & t_d &= \max\left\{m_{B_c}\sqrt{|\alpha_d|}, m_{B_c}\sqrt{|\beta_d|}, 1/b_1, 1/b\right\}, \\
t_e &= \max\left\{m_{B_c}\sqrt{|\alpha_e|}, m_{B_c}\sqrt{|\beta_e|}, 1/b_3, 1/b_1\right\}, & t_f &= \max\left\{m_{B_c}\sqrt{|\alpha_f|}, m_{B_c}\sqrt{|\beta_f|}, 1/b_3, 1/b_1\right\}, \\
t_g &= \max\left\{m_{B_c}\sqrt{|\alpha_g|}, m_{B}\sqrt{|\beta_g|}, 1/b_3, 1/b\right\}, & t_h &= \max\left\{m_{B_c}\sqrt{|\alpha_h|}, m_{B_c}\sqrt{|\beta_h|}, 1/b, 1/b_3\right\},
\end{aligned} \tag{A2}
$$

where

$$
\begin{aligned}
&\alpha_a = r_b^2 + (1-r^2)[(\eta-1)x_3 - \eta], && \beta_a = (r^2 - x_B)[(1-\eta)(x_3-1) + x_B],\\
&\alpha_b = (r^2 - x_B)(x_B + \eta - 1), && \beta_b = \beta_a,\\
&\alpha_c = \beta_a, && \beta_c = [1 - x_B - (1-r^2)z][(1-\eta)x_3 + x_B - 1],\\
&\alpha_d = \beta_a, && \beta_d = [(1-z)r^2 - x_B + z][(1-\eta)(x_3-1) + x_B],\\
&\alpha_e = (1-\eta)(r^2-1)x_3 z, && \beta_e = r_b^2 - [(1-r^2)z + x_B - 1][(1-\eta)x_3 + x_B - 1],\\
&\alpha_f = \alpha_e, && \beta_f = r_c^2 - [(r^2-1)z + x_B][(\eta-1)x_3 + x_B],\\
&\alpha_g = (1-r^2)[(\eta-1)x_3 - \eta], && \beta_g = \alpha_e,\\
&\alpha_h = r_c^2 + (1-\eta)[r^2(z-1) - z], && \beta_h = \alpha_e.
\end{aligned}
\tag{A3}
$$

The Sudakov factors can be written as

$$
\begin{aligned}
S_{ab}(t) &= s\left(\frac{m_{B_c}}{\sqrt{2}}x_B, b_1\right) + s\left(\frac{m_{B_c}}{\sqrt{2}}x_3, b_1\right) + \frac{5}{3}\int_{1/b_1}^{t}\frac{d\mu}{\mu}\gamma_q(\mu) + 2\int_{1/b_3}^{t}\frac{d\mu}{\mu}\gamma_q(\mu),\\
S_{cd}(t) &= s\left(\frac{m_{B_c}}{\sqrt{2}}x_B, b_1\right) + s\left(\frac{m_{B_c}}{\sqrt{2}}z, b\right) + s\left(\frac{m_{B_c}}{\sqrt{2}}(1-z), b\right) + s\left(\frac{m_{B_c}}{\sqrt{2}}x_3, b_1\right) + \frac{11}{3}\int_{1/b_1}^{t}\frac{d\mu}{\mu}\gamma_q(\mu) + 2\int_{1/b}^{t}\frac{d\mu}{\mu}\gamma_q(\mu),\\
S_{ef}(t) &= s\left(\frac{m_{B_c}}{\sqrt{2}}x_B, b_1\right) + s\left(\frac{m_{B_c}}{\sqrt{2}}z, b_3\right) + s\left(\frac{m_{B_c}}{\sqrt{2}}(1-z), b_3\right) + s\left(\frac{m_{B_c}}{\sqrt{2}}x_3, b_3\right) + \frac{5}{3}\int_{1/b_1}^{t}\frac{d\mu}{\mu}\gamma_q(\mu) + 4\int_{1/b_3}^{t}\frac{d\mu}{\mu}\gamma_q(\mu),\\
S_{gh}(t) &= s\left(\frac{m_{B_c}}{\sqrt{2}}z, b\right) + s\left(\frac{m_{B_c}}{\sqrt{2}}(1-z), b\right) + s\left(\frac{m_{B_c}}{\sqrt{2}}x_3, b_3\right) + 2\int_{1/b}^{t}\frac{d\mu}{\mu}\gamma_q(\mu) + 2\int_{1/b_3}^{t}\frac{d\mu}{\mu}\gamma_q(\mu).
\end{aligned}
\tag{A4}
$$

As we know, the double logarithms $\alpha_s \ln^2 x$ produced by the radiative corrections are not small expansion parameters when the end point region is important; in order to improve the perturbative expansion, the threshold resummation of these logarithms to all orders is needed, which leads to a quark jet function

$$
S_t(x) = \frac{2^{1+2c}\Gamma(3/2+c)}{\sqrt{\pi}\Gamma(1+c)}[x(1-x)]^c, \tag{A5}
$$

with $c = 0.3$. It is effective to smear the end point singularity with a momentum fraction $x \to 0$.

[1] R. Aaij *et al.* (LHCb Collaboration), Phys. Rev. D **94**, 091102 (2016).
[2] R. Aaij *et al.* (LHCb Collaboration), Phys. Rev. D **95**, 032005 (2017).
[3] R. Aaij *et al.* (LHCb Collaboration), Phys. Lett. B **759**, 313 (2016).
[4] R. Aaij *et al.* (LHCb Collaboration), J. High Energy Phys. 01 (2022) 065.
[5] B. Bhattacharya, M. Gronau, and J. L. Rosner, Phys. Lett. B **726**, 337 (2013).
[6] M. Gronau, Phys. Lett. B **727**, 136 (2013).
[7] D. Xu, G. N. Li, and X. G. He, Phys. Lett. B **728**, 579 (2014).
[8] M. Gronau and J. L. Rosner, Phys. Rev. D **72**, 094031 (2005).
[9] G. Engelhard and G. Raz, Phys. Rev. D **72**, 114017 (2005).
[10] M. Imbeault and D. London, Phys. Rev. D **84**, 056002 (2011).
[11] X. G. He, G. N. Li, and D. Xu, Phys. Rev. D **91**, 014029 (2015).
[12] S. H. Zhou, R. H. Li, Z. Y. Wei, and C. D. Lu, Phys. Rev. D **104**, 116012 (2021).
[13] S. Kränkl, T. Mannel, and J. Virto, Nucl. Phys. **B899**, 247 (2015).
[14] H. Y. Cheng, C. K. Chua, and Z. Q. Zhang, Phys. Rev. D **94**, 094015 (2016).
[15] Y. Li, Phys. Rev. D **89**, 094007 (2014).
[16] H. Y. Cheng, C. K. Chua, and A. Soni, Phys. Rev. D **76**, 094006 (2007).

[17] R. Klein, T. Mannel, J. Virto, and K. K. Vos, J. High Energy Phys. 10 (2017) 117.
[18] Y. C. Zhao, Z. Q. Zhang, Z. Y. Zhang, Z. J. Sun, and Q. B. Meng, Chin. Phys. C **47**, 073104 (2023).
[19] Z. Q. Zhang, Y. C. Zhao, Z. L. Guan, Z. J. Sun, Z. Y. Zhang, and K. Y. He, Chin. Phys. C **46**, 123105 (2022).
[20] Z. Q. Zhang and H. Guo, Eur. Phys. J. C **79**, 59 (2019).
[21] Y. Li, W. F. Wang, A. J. Ma, and Z. J. Xiao, Eur. Phys. J. C **79**, 37 (2019).
[22] A. J. Ma, Y. Li, and Z. J. Xiao, Nucl. Phys. **B926**, 584 (2018).
[23] C. H. Chen and H.-n. Li, Phys. Rev. D **70**, 054006 (2004).
[24] C. H. Chen and H.-N. Li, Phys. Lett. B **561**, 258 (2003).
[25] X. Liu, H.-n. Li, and Z. J. Xiao, Phys. Rev. D **97**, 113001 (2018).
[26] T. W. Chiu, T.-H. Hsieh, C.-H. Huang, and K. Ogawa (TWQCD Collaboration), Phys. Lett. B **651**, 171 (2007).
[27] H.-n. Li, Y. L. Shen, and Y. M. Wang, J. High Energy Phys. 02 (2013) 008.
[28] H.-n. Li and Y. M. Wang, J. High Energy Phys. 06 (2015) 013.
[29] T. Kurimoto, H.-n. Li, and A. I. Sanda, Phys. Rev. D **67**, 054028 (2003).
[30] R. H. Li, C. D. Lu, and Z. Hao, Phys. Rev. D **78**, 014018 (2008).
[31] A. J. Ma, Y. Li, W. F. Wang, and Z. J. Xiao, Phys. Rev. D **96**, 093011 (2017).
[32] A. J. Ma, W. F. Wang, Y. Li, and Z. J. Xiao, Eur. Phys. J. C **79**, 539 (2019).
[33] R. Aaij *et al.* (LHCb Collaboration), Phys. Rev. D **92**, 012012 (2015).
[34] R. Aaij *et al.* (LHCb Collaboration), Phys. Rev. D **94**, 072001 (2016).
[35] R. Aaij *et al.* (LHCb Collaboration), Phys. Rev. D **91**, 092002 (2015).
[36] G. Buchalla, A. J. Buras, and M. E. Lautenbacher, Rev. Mod. Phys. **68**, 1125 (1996).
[37] T. Feldmann, P. Kroll, and B. Stech, Phys. Rev. D **58**, 114006 (1998).
[38] R. L. Workman *et al.* (Particle Data Group), Prog. Theor. Exp. Phys. **2022**, 083C01 (2022).
[39] M. Cepeda, S. Gori, P. Ilten, M. Kado, F. Riva, R. Abdul Khalek, A. Aboubrahim, J. Alimena, S. Alioli, A. Alves *et al.*, CERN Yellow Rep. Monogr. **7**, 221 (2019).
[40] Z. Rui, Z. T. Zou, and C. D. Lu, Phys. Rev. D **86**, 074008 (2012).
[41] X. Liu, Z. J. Xiao, and C. D. Lu, Phys. Rev. D **81**, 014022 (2010).
[42] J. F. Liu and K. T. Chao, Phys. Rev. D **56**, 4133 (1997).
[43] H. M. Choi and C. R. Ji, Phys. Rev. D **80**, 114003 (2009).
[44] H. F. Fu, Y. Jiang, C. S. Kim, and G. L. Wang, J. High Energy Phys. 06 (2011) 015.
[45] S. D. Genon, J. He, E. Kou, and P. Robbe, Phys. Rev. D **80**, 114031 (2009).
[46] J. Chai, S. Cheng, Y. H. Ju, D. C. Yang, C. D. Lu, and Z. J. Xiao, Chin. Phys. C **46**, 123103 (2022).
[47] H. Y. Cheng and C. K. Chua, Phys. Rev. D **80**, 114008 (2008).
[48] W. Wang, Y. M. Wang, D. S. Yang, and C. D. Lu, Phys. Rev. D **78**, 034011 (2008).